Supplementary Information

A flame-retardant polymer electrolyte for high performance lithium metal batteries with an expanded operation temperature

Jingwei Xiang,‡[a] , Yi Zhang,‡[a], Bao Zhang,[b] Lixia Yuan,*[a] Xueting Liu,[a] Zexiao Cheng,[a] Yan Yang,[a] Xinxin Zhang,[a] Zhen Li,[a] Yue Shen,[a] Jianjun Jiang,[b] Yunhui Huang,*[a]

a. State Key Laboratory of Material Processing and Die & Mold Technology, School of Materials Science and Engineering, Huazhong University of Science and Technology, Wuhan, Hubei 430074, China

b. School of Optical and Electronic Information, Huazhong University of Science and Technology, Wuhan, Hubei 430074, China

‡These authors contributed equally to this work.

*Corresponding authors: yuanlixia@hust.edu.cn, huangyh@hust.edu.cn

Methods

Preparation of PDE. The precursor solvent for PDE was prepared by dissolving 2M LiTFSI in DOL in an argon-filled glove box (H_2O < 0.1 ppm, O_2 < 0.1 ppm) at room temperature. Then 1 wt%, 3 wt% and 5 wt% TB were added to the precursor solution, respectively, and stirred until completely dissolved. The prepared solvents spontaneously converted to PDE after resting for 12 h at room temperature.

Ultrasonic imaging. Ultrasonic transmission mappings are acquired by an ultrasonic battery scanner (UBSC-LD50 from Jiangsu Jitri-Hust Intelligent Equipment Technology Co., Ltd)[53]. Firstly, the pouch cell was clamped to the test clips and fully immersed in the silicone oil-filled test tank. Then a pair of ultrasonic focusing transducers (30 mm focal distance, 2 MHz frequency) were placed on each side of the pouch cell. Ultrasound waves are emitted from a focused transducer on one side and penetrate the cell, where they are subsequently received by a transducer on the other side. Then transmitted waveforms were collected with a data acquisition card and the peak-to-peak values of the acquired transmission waves were converted to a color scale to obtain a pseudo-color image.

Electrochemical measurements. All batteries were assembled in an argon-filled glove box (H_2O < 0.1 ppm, O_2 < 0.1 ppm) and the in-situ formed polymer batteries were tested after 14 h of resting. The Li|Cu and Li|Li batteries were assembled to measure the CE and the stability of the electrolyte with Li metal anode, respectively. The charging-discharging tests were performed on a Neware electrochemical testing system. The LSV measurements were conducted via Li|stain steel cells on an electrochemical workstation (CHI660E, Shanghai Chen Hua). The Li-ion transference numbers of electrolytes were measured by chronoamperometry using Li|Li symmetric coin cells at room temperature. The S cathode was prepared by casting the homogeneous slurry of S, conductive carbon and polyvinylidene fluoride (PVDF) with a mass ratio of 6:3:1 on a carbon-coated Al foil. Then the electrode was dried in a

vacuum oven at 80 ºC for 24 h. The low sulfur loading of each cathode was 0.5 ~ 1 mg cm^{-2} and the high S loading of the cathode was 4 mg cm^{-2}. The NCM_{622} and $LiFeO_4$ cathodes were fabricated by mixing the NCM_{622} and $LiFeO_4$ with conductive carbon and PVDF in a mass ratio of 8:1:1. Then the slurries were immobilized on carbon-coated Al foils and dried for 24 h at 80 ºC in a vacuum oven. The $LiFeO_4$ and NCM_{622} loadings of each cathode were ~ 1 mg cm^{-2} and ~ 4 mg cm^{-2}. Cycling performances of Li-S, Li-NCM_{622} and Li-$LiFeO_4$ were measured on a Neware electrochemical testing system.

Material characterizations. ^{1}H NMR and ^{13}C NMR spectra of the electrolytes were measured on a Bruker 400 MHz NMR spectrometer with dimethyl sulfoxide-d_6 as the deuterated solvent. The morphologies of the Li metal anode and cathodes were characterized on a field-emission SEM (SIRION200). FTIR spectra of the electrolytes were conducted on a Bruker Vertex 70 FTIR spectrometer. X-ray photoelectron spectroscopy (XPS; AXIS ULTRA DLD-600W) were used to analysis the composition information of the SEI.

Molecular dynamics simulations. Molecular dynamics (MD) simulations were performed to investigate the structures of electrolyte. The MD simulations were run using LAMMPS[1]. The systems are setup initially by using PACKMOL[2] and Moltemplate (http://www.moltemplate.org/). Periodic boxes were used here. The force-fields parameters of Li^+ and $TFSI^-$ are taken from previous publications[3,4]. The force-fields parameters of DOL and poly-DOL are taken from OPLS-AA parameters[5]. Herein, an oligomer ($[C_2H_5OCH_2O]_{10}H$) form was utilized to simplify the polymer electrolyte simulations. The force-fields parameters of $B(C_6F_5)_3$ are taken from Universal Force Field[6].

First, NPT simulations were performed at 298 K for 5 ns. The NPT runs were controlled by Nose-Hoover thermostat and barostat with a 100fs damping parameter. Then, the NVT runs were 10 ns long at 298K. At this state, all simulated systems were surely equilibrated.

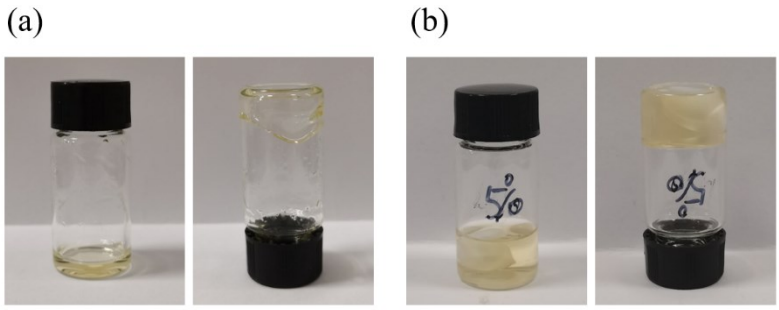

Supplementary Fig. 1 Digital photographs of 1TB-PDE (a) and 5TB-PDE (b).

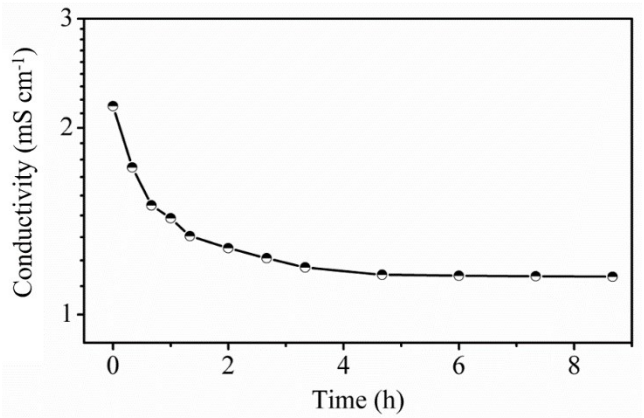

Supplementary Fig. 2 Conductivity versus polymerization time for PDE.

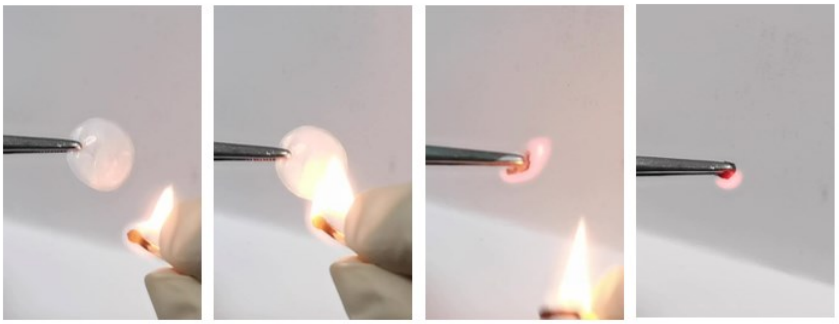

Supplementary Fig. 3 Flame test of the separator with PEO electrolyte infiltration.

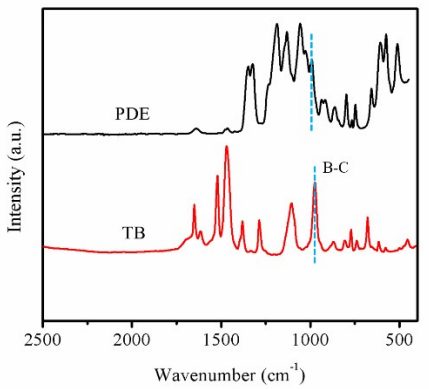

Supplementary Fig. 4 FTIR spectra of PDE and TB.

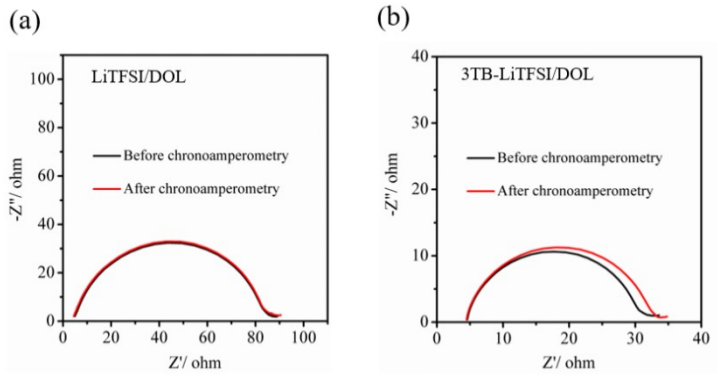

Supplementary Fig. 5 Nyquist plots of LDE (a) and PDE (b).

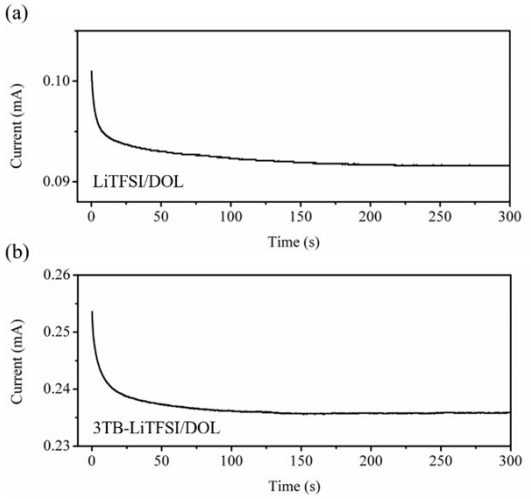

Supplementary Fig. 6 Amperometric i-t curves of LDE (a) and PDE (b).

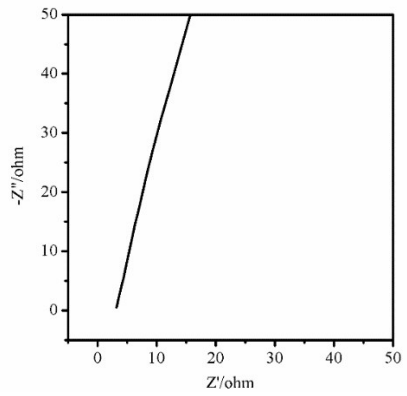

Supplementary Fig. 7 Electrochemical impedance spectroscopy of PDE at room temperature.

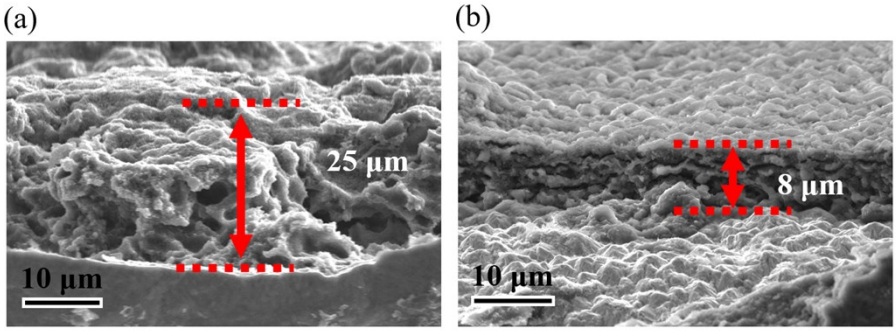

Supplementary Fig. 8 Cross-section SEM images of deposited Li on Cu foils with LDE and PDE after 100 cycles at 0.5 mA cm^{-2} for 0.5 mAh cm^{-2}.

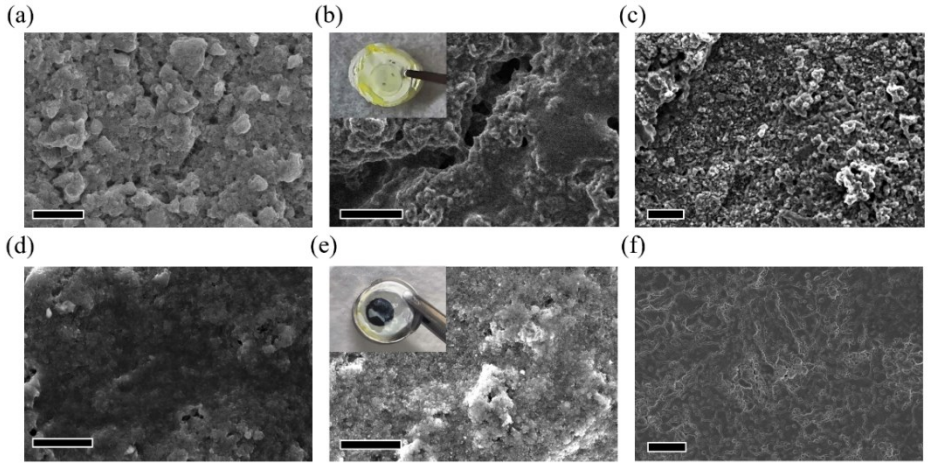

Supplementary Fig. 9 SEM images of S cathodes before (a, d) and after (b, e) cycles in LDE (d, e) and PDE (a, b), SEM images of Li metal anodes after cycles in LDE (f) and PDE.

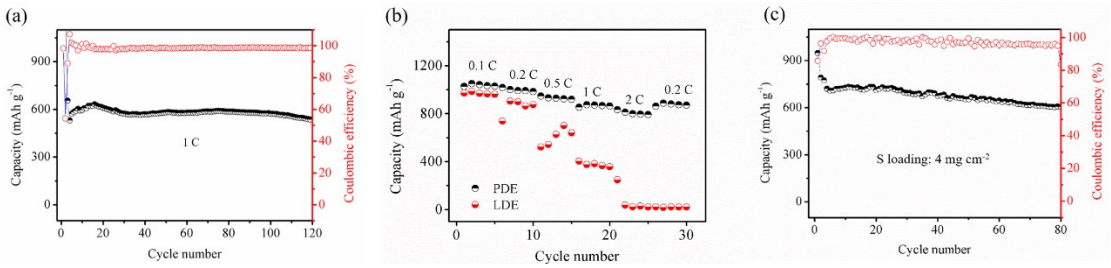

Supplementary Fig.10 a. The cycling performance and CE of Li-S battery at 1 C, b. Rate performances of batteries using PDE and LDE, c. The cycling performance of Li-S battery with PDE of high S loading (4 mg cm^{-2}).

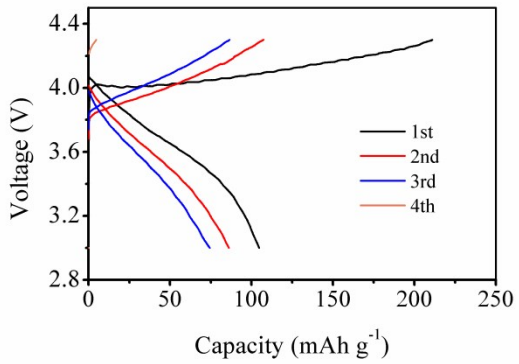

Supplementary Fig. 11 Charge/discharge profiles of NCM_{622}-Li battery in LDE at 0.5 C.

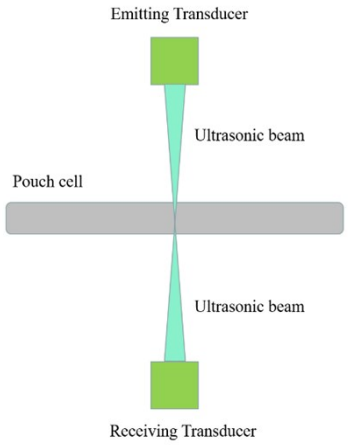

Supplementary Fig. 12 A diagram of the path of the focused ultrasonic beam.

Supplementary Fig. 13 The Optical image of an ultrasonic battery scanner.

References

1 Plimpton, S. Fast parallel algorithms for short-range molecular dynamics. *J. Comput. Phys.* **117**, 1–19 (1995).

2 Martínez, L., Andrade, R., Birgin, E.G., Martínez, J. M. PACKMOL: a package for building initial configurations for molecular dynamics simulations. *J. Comput. Chem.* **30**, 2157–2164 (2009).

3 Canongia Lopes, J.N., Pádua, A.A.H. Molecular force field for ionic liquids composed of triflate or bistriflylimide snions. *J. Phys. Chem. B* **108**, 16893–16898 (2004).

4 Kumar, N., Seminario, J.M. Lithium-ion model behavior in an ethylene carbonate electrolyte using molecular dynamics. *J. Phys. Chem. C* **120**, 16322–16332 (2016).

5 Jorgensen, W.L., Maxwell, D.S., Tirado-Rives, J. Development and testing of the OPLS all-atom force field on conformational energetics and properties of organic liquids. *J. Am. Chem. Soc.* **118**, 11225–11236 (1996).

6 Rappé, A.K., Casewit, C.J., Colwell, K.S., Goddard III, W.A., Skiff, W.M. UFF, a full periodic table force field for molecular mechanics and molecular dynamics simulations. *J. Am. Chem. Soc.* **114**, 10024–10035 (1992).